New kiln technology expands market opportunities for cryptocrystalline magnesite

John Keeling[1], Ric Horn[2] and Ian Wilson[3]

1 Geological Survey of South Australia, Department for Energy and Mining
2 Hornet Resource Assessment Services Pty Ltd
3 Industrial Minerals Consultant, Cornwall, UK

Introduction

In 2013 Australian startup, Calix Limited, built and commissioned a commercial-scale demonstrator plant at Bacchus Marsh, Victoria, based on their patented technology, to showcase a transformational calcination process for creating reactive oxide products whilst also capturing carbon dioxide (CO_2) released during the reaction. Integral to the successful commercial introduction of the technology was the quality of reactive magnesium oxide (magnesia, MgO) product achieved using cryptocrystalline magnesite ($MgCO_3$) from the Myrtle Springs mine in South Australia. Calix has successfully marketed the product, as a magnesium hydroxide ($Mg(OH)_2$) slurry, for pH and odour control in sewer and wastewater industries and as an effective coating for protection of sewer concrete infrastructure against acid corrosion. New applications in aquaculture and agriculture are currently under evaluation, with field trials in Australia and overseas. Research projects are underway also into products for the health and pharmaceutical sectors, 3D printing, advanced building materials and catalysts (Calix 2018). Magnesia with a very high surface area underpins much of this activity. The relative contributions from characteristics specific to the raw magnesite feedstock and those from refinements to the kiln operating conditions to create the highly reactive MgO product are the subject of ongoing investigation. In this regard, the occurrence and properties of marine sedimentary magnesite from the northern Flinders Ranges are somewhat unique amongst global magnesite deposits.

Of equal or greater significance for the Calix kiln technology is the effective capture of pure CO_2 released during calcination. This aspect has attracted international interest, with European cement and lime producers partnering with Calix in the design and build of a demonstration plant at HeidelbergCement's Lixhe cement plant in Belgium. Total emissions from cement manufacture constitute ~8% of global anthropogenic CO_2 emissions (Olivier et al. 2016). Over the next two years, the Calix kiln technology will be fully tested and evaluated as a key component of the LEILAC (Low Emissions Intensity Lime and Cement) project to largely eliminate CO_2 process emissions from cement and lime manufacture as an important contribution towards the EU target of cutting CO_2 emissions to 80% below 1990 levels by 2050 (LEILAC 2017).

The significance of the new technology for further development of South Australian magnesite resources is considered here in the context of:

- global magnesite markets and sources
- geology and characteristics of sedimentary magnesite deposits of the northern Flinders and Willouran ranges
- previous work to evaluate and develop the sedimentary magnesite resources
- history of development of the Calix kiln technology
- new market opportunities for cryptocrystalline magnesite.

Magnesite markets and sources

The main driver of magnesite markets over many decades has been the refractories industry where magnesite is used to produce magnesia (MgO) as the principal component of basic refractory formulations used to line furnaces in the steel industry, and for heat containment in some areas of cement, non-ferrous metal and glass manufacture. For refractory markets, magnesia is produced as dead-burned magnesia (DBM; 1,500–2,300 °C; 93–99.8% MgO) and fused magnesia (FM; 2,800–3,000 °C; 97–99.8% MgO) where purity, high-temperature treatment, increased density, coarse crystal size and low reactivity equate with increased performance and price (Table 1).

Table 1 *Magnesite and magnesia markets*

Magnesite ($MgCO_3$)/magnesia (MgO) markets → increasing heat treatment and price/tonne			
$MgCO_3$	MgO		
Raw magnesite	Caustic calcined magnesia (CCM)	Dead-burned magnesia (DBM)	Fused magnesia (FM)
	700–1,500°C	1,500–2,300°C	2,800–3,000°C
		Refractory grade 93, 95, 97% MgO	Refractory/electrical grade >97% MgO
Mg metal Agriculture • soil pH • animal feed • fertiliser Fillers Ceramics Surface coating Pesticide carrier Decorative	Feedstock for DBM, FM refractories Environmental • wastewater treatment • flue gas treatment Agriculture • fertiliser • pesticide • animal feed Aquaculture Magnesia cements • concrete floors, blocks, wall panels • insulation panels Fillers Flame retardant	Refractories • bricks • castables • gunning mixtures Welding flux Magnesia phosphate cement	Refractory bricks Transformer steel coatings Cable insulation Electrical elements Hi-tech ceramics

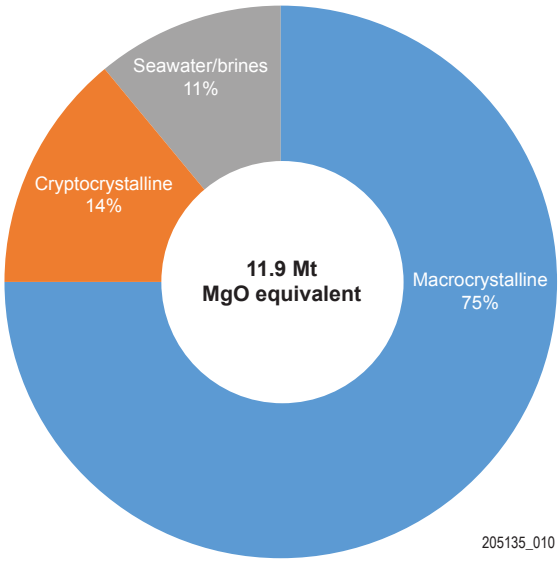

Figure 1 *World magnesia production capacity in 2017 by source contribution. (Source: O'Driscoll 2018)*

Magnesia is produced largely by the calcination of natural minerals (~89%), principally magnesite, and rarely from brucite ($Mg(OH)_2$), dolomite ($CaMg(CO_3)_2$) or hydromagnesite ($Mg_5(CO_3)_4(OH)_2{\cdot}4H_2O$). About 11% is produced synthetically by calcination of $Mg(OH)_2$ derived as a precipitate from seawater and brines (Fig. 1).

The temperature of calcination influences the crystal size and reactivity of the MgO product. Caustic calcined magnesia (CCM; 700–1,500 °C) is most reactive and is the primary feedstock for DBM and FM manufacture, although an increasing proportion (currently 20–30%) is used also in other markets including magnesium cements, agriculture, animal feed supplements, wastewater treatment and acid neutralisation (Table 1). Non-refractory magnesia markets in 2017 were estimated to exceed 4 Mt (Wietlisbach 2018). Comparatively smaller amounts of natural magnesite are crushed and milled for use as an industrial mineral filler, as soil fertiliser and for acid neutralisation.

Magnesite production worldwide in 2018 was ~29 Mt (United States Geological Survey 2019) with ~64% from deposits in China (Fig. 2). Tightening of environmental regulations in China, including restrictions on the use of explosives and stricter limits for kiln emissions, has required some rationalisation of magnesite mining and processing resulting in reduced supply for refractory markets leading to price increases (Flook and Wilson 2016; O'Driscoll 2018). This has led to increased output from some European operations and prompted reassessment of alternative sources of supply. Australian production in 2017 was just under 500,000 t of cryptocrystalline magnesite, principally from the Kunwarwara deposits in Queensland, with minor production also from Myrtle Springs in South Australia and Thuddungra in New South Wales. There was renewed interest also in development of known macrocrystalline magnesite resources in the Northern Territory (Huandot, Winchester) and Tasmania (Arthur River, Lyons River) (Perks 2017).

World magnesite resources are large at >13,000 Mt (Wilson 2010) with the bulk of reserves located in China (26%), Russia (23%) and North Korea (21%), followed by Slovakia, Brazil, Australia, Turkey, Greece, India and Austria, contributing from 9% to 3%, and others at <2% (Flook and Wilson 2016). Most of the resources (90%) are carbonate-hosted, fine- to coarse-grained macrocrystalline magnesite termed 'sparry' or 'phanerocrystalline' magnesite; the remaining 10% are fine-grained 'cryptocrystalline' magnesite, also referred to as 'amorphous' magnesite. The latter form by

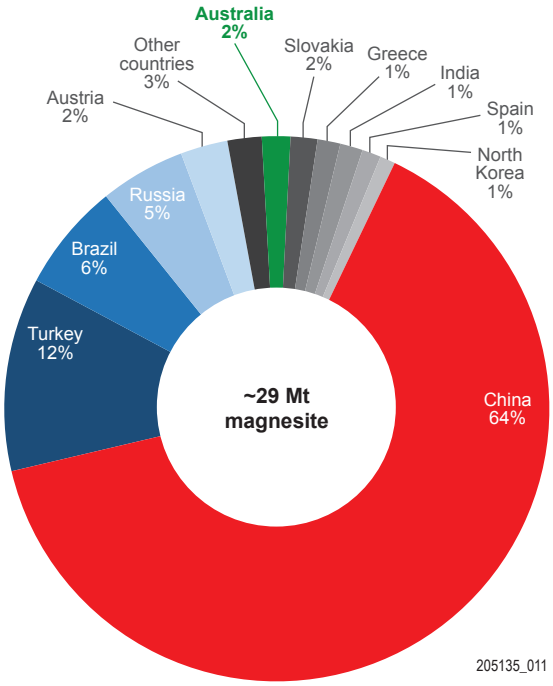

Figure 2 Proportion of world magnesite production in 2018 by country. (Source: United States Geological Survey 2019)

hydrothermal or supergene alteration of ultramafic rocks, as continental sedimentary lacustrine deposits, and rarely as Proterozoic shallow marine evaporite deposits.

Macrocrystalline magnesite

The giant macrocrystalline magnesite deposits of China are Paleoproterozoic age and are distributed along the Haicheng-Diashiqiao talc-magnesite ore belt, mostly within Liaoning Province in northeastern China. Mining operations and magnesia production are concentrated in centres Dashiqiao, Haicheng, Xiuyan and Fengcheng. The talc-magnesite belt trends roughly E–W and extends for ~100 km over an average width of 4 km. Medium to coarse crystalline magnesite deposits range from 200 to 2,700 m in length and 30–300 m thickness (Jiang et al. 2004). The magnesite deposits are hosted by metamorphic rocks that were originally sediments deposited in an intracontinental rift as part of a marine carbonate package with magnesite concentrated in the upper Dashiqiao Formation. Depositional environment was carbonate platform through to shallow coastal lagoons with some primary magnesite sedimentation under evaporative conditions (Dong et al. 2016). Rifting and sedimentation ceased in the late Paleoproterozoic with the onset of the Lüliang compressional event (pre-1869 ± 7Ma), which resulted in folding of the Dashiqiao Formation and regional metamorphism at upper greenschist to amphibolite facies. Tectonic reactivation occurred during the Mesozoic Yanshanian orogeny and was accompanied by multiple thermal events with intense magmatism and lamprophyre dyke intrusions, indicative of lithospheric thinning (Jiang et al. 2005). Preservation of rare magnesite stromatolites provide evidence of at least some primary sedimentary magnesite, but the Dashiqiao Formation carbonates were modified extensively by metasomatic alteration due to mobilisation and infiltration of magnesium-rich brines (Chen et al. 2002; Jiang et al. 2004; Dong et al. 2016), by recrystallisation during regional metamorphism, and by later hydrothermal fluids associated with the Mesozoic igneous activity (Mish et al. 2018). Other large macrocrystalline magnesite deposits in Russia, North Korea, Austria and Brazil show similarities in their style of formation, in particular the rift basin setting, evidence of marine lagoonal evaporite facies, and post-burial magnesian metasomatism of precursor magnesium-rich carbonate rocks (Pohl 1990; Ebner et al. 2004; Parente et al. 2004; Zadeh, Ebner and Jiang 2015; Krupenin and Kol'tsov 2017).

Cryptocrystalline magnesite

Cryptocrystalline magnesite deposits are generally smaller and shallower compared with macrocrystalline magnesite. They are characterised by very fine grained magnesite crystals, typically 1 to 10 μm across, which gives a high surface area and high reactivity. Important deposit styles include magnesite stockworks and veins formed during weathering or hydrothermal alteration of ultramafic rocks, and continental lacustrine chemical sediments resulting from groundwater mixing or evaporation of magnesium-rich waters.

Australia's largest magnesite mining operation, near Kunwawara, extracts cryptocrystalline magnesite from Cenozoic (post Eocene) fluvial channel deposits formed in areas draining weathered ultramafic rocks. The fluvial deposits are overlain by extensive thin cover of 1–4 m thickness of sheetflood black clay alluvium. Magnesite nodules formed through cyclic processes of evaporation, concentration and precipitation of hydrated magnesium-carbonate from magnesium-rich groundwater. These processes were concentrated at or near the watertable during fluvial sediment accumulation within a channel that is 0.5–3 km wide and over 30 km long (Wilcock 1998; Department of Natural Resources and Mines, Queensland 2017). The channel fill varies from 10–40 m thickness and consists of gravel and coarse sand at the base grading upwards to fine sand, siltstone and claystone. Magnesite nodules with low iron oxide content (<0.3%) are concentrated in weakly cemented fine sand and siltstone forming the upper half of the sequence. Magnesite makes up 5–95% of the sediment, but averages 35% and 12 m thickness in areas selected for mining (Wilcock

1998). The nodules range from a few millimetres to 600 mm in size. Minor impurities include dolomite, silica, clay, iron and manganese oxides, which tend to be concentrated with amorphous silica forming an outer skin on dense high-purity bone magnesite nodules, or are more pervasive in less-dense chalky nodules and veins (Milburn and Wilcock 1998). Annual production of ~3 Mt of magnesite ore is dug using hydraulic excavators, with no requirement for blasting. Mined ore is beneficiated in a two-stage process. Wet screening is used to separate the magnesite nodules; under 20 mm is rejected as waste, 20–63 mm is stockpiled, and over 63 mm is crushed and stockpiled separately. The ore is then treated by scrubbing and wet screening, with heavy media (ferro-silicon) drum separation to remove sandstone fragments, followed by crushing, screening and hydrocyclone heavy media (ferro-silicon) separation to split grades by density (Hill 1992). Chemical testing and blending from stockpiles is done prior to transport, 65 km south, to Sibelco Ltd's Parkhurst plant at Rockhampton for calcining. At Parkhurst, various magnesia products are made, including CCM using gas-fired multiple hearth furnaces operating to 1,000 °C, DB from selected CCM finely ground, pressed into briquettes and fired at up to 2,300 °C in high-temperature gas fired shaft kilns, and FM from high-grade magnesia melted at 2,800–3,000 °C in electric arc furnaces (Queensland Metals Corporation Ltd 1996). The plant has capacity to produce 320,000 tpa CCM, 110,000 tpa DB and 32,000 tpa FM. Output and product mix is flexible and reflects market demand, price and cost of production.

Turkey is the largest producer of cryptocrystalline magnesite from extensive stockwork and vein deposits within areas of serpentinised Cretaceous ultramafic rocks incorporated within early Cenozoic ophiolite complexes of the Alpine orogenic belt in the west and northeast of the country. Deposits are characterised by abundant centimetre–sized veins and veinlets of magnesite in serpentine host, along with larger veins to 4 m width within structurally controlled faults and fractures. Alteration of serpentine ($Mg_3Si_2O_5(OH)_4$) provides the source of magnesium. Carbon isotope studies indicate CO_2 is derived primarily from oxidation of organic-rich metasediments, underthrust at depth, together with a smaller contribution from atmospheric CO_2 as bicarbonate circulated in heated meteoric water (Zedef, Russell and Fallick 2000). Kümaş Manyezit Sanayi AS is the leading producer with 160 Mt resource contained in deposits at Eskişehir, Bilecik and Kütahya in northwest Turkey and processed predominantly at the Kütahya plant; MgO production capacity is 400,000 tpa, of a total Turkish production of ~900,000 tpa MgO. Run-of-mine ore contains ~25% $MgCO_3$ which is beneficiated by processes involving hand sorting, crushing and screening to give a 20–40 mm feed for magnetic separation to remove serpentinite/magnetite followed by washing, and further crushing, drying and magnetic separation, with a final upgrade using optical colour sorting. The low-silica product is calcined using mostly rotary kilns to produce a high-quality DBM for refractory brick and monolithic manufacture. Selected high-grade MgO is used in FM production for refractories and for electrical insulators in heating elements.

Synthetic magnesium hydroxide

Synthetic $Mg(OH)_2$ from seawater and brines provides feedstock for around 11% of magnesia production, with largest operations located in Japan, United States, Ireland, Israel and Jordan. Seawater contains ~0.13% Mg as Mg^{2+} and $MgSO_4$; Mg is extracted as insoluble precipitate $Mg(OH)_2$ by the addition of hydrated lime (CaO) or dolime (CaO·MgO), via the reactions:

$$CaO + H_2O + MgCl_2 \rightarrow Mg(OH)_2\downarrow + CaCl_2$$

$$CaO{\cdot}MgO + 2H_2O + MgCl_2 \rightarrow 2Mg(OH)_2\downarrow + CaCl_2$$

Prior to the addition of alkali, pre-treatment of seawater is necessary including filtration to remove suspended solids, chlorination to prevent marine algal growth, and acidification to remove any CO_2 present as soluble bicarbonate. Removal of bicarbonate prevents precipitation of insoluble $CaCO_3$ with $Mg(OH)_2$ and is achieved by the addition of concentrated sulfuric acid to levels of pH <4 followed by aeration to release the CO_2. The crystal size and purity of the $Mg(OH)_2$ precipitate is influenced by the quality of the calcined limestone or dolomite, the temperature of calcination, and the rate of addition to seawater in order to maintain the level of alkalinity necessary to achieve the desired crystal growth rate and morphology (Shand 2006). Seawater also contains boron as boric acid (H_2BO_3) at levels of ~4.6 ppm B, which is preferentially adsorbed on the charged surface of crystallising $Mg(OH)_2$ particles. The presence of boron in MgO is undesirable for refractory products as it reduces the melting point and lowers performance under high-temperature operation. Boron adsorption can be reduced to <300 ppm in MgO product by over-liming seawater to increase the pH, but this needs to be balanced with the tendency for excess calcium to precipitate with $Mg(OH)_2$ (Shand 2006). Precipitates of $Mg(OH)_2$ are thickened, filtered and washed before being converted to MgO in multiple hearth furnaces over the temperature range 400–900 °C.

Seawater magnesia is used for production of refractory DBM and FM, including high performance electrical grade FM. Additional uses are in the production of magnesium chemicals, pharmaceuticals, ceramics and magnesium metal.

Geology of Neoproterozoic sedimentary magnesite in the northern Flinders and Willouran ranges

In South Australia, magnesite is widespread as a minor component of Neoproterozoic shallow marine carbonates of Skillogalee Dolomite of the Mundallio Subgroup of Burra Group sediments deposited in fault-bounded sub-basins during renewed rifting and widening of the Adelaide Geosyncline, post 800 Ma (Belperio 1990; Preiss 2000). In the northern Flinders Ranges, Skillogalee Dolomite conformably overlies Copley Quartzite, a fluvial sandstone member of the Emeroo Subgroup, and is in turn overlain by shallow marine siltstone and dolomite of Myrtle Springs Formation. Volcaniclastic interbeds in the lower portion of Skillogalee Dolomite at Burra were dated at c. 790 Ma (U–Pb zircon) (Preiss, Drexel and Reid 2009). Magnesite is concentrated in the upper part of Skillogalee Dolomite mostly as thin intraclastic beds of mud-pellet conglomerate, rarely as finely bedded micritic magnesite, repetitively interbedded with cryptalgal finely laminated micritic dolomite, dolomitic stromatolites (*Baicalia burra*), pelletal dolomite and dolomite grainstone, with minor quartzose siltstone and sandstone. Cumulative thickness of magnesite was greatest along the western margin of the northern Flinders Ranges extending for ~120 km NW of Leigh Creek into the Willouran Ranges (Fig. 3). Here magnesite beds ranging from a few centimetres to several metres thickness may comprise >20% of the sedimentary package over intervals exceeding 100 m.

Sedimentary structures and chemical indicators from sequences containing magnesite are consistent with a depositional environment that was shallow marine to peritidal with frequent subaerial exposure and depth of water that rarely exceeded a few metres. Micritic dolomite with fine organic laminae and intraformational cryptalgal dolomite, together with tepee structures and mudcracks, are characteristic of shallow subtidal deposits and mudflats exposed to drying and reworking (Belperio 1990). Magnesite interbeds in Skillogalee Dolomite are almost exclusively reworked (Fig. 4), but rare, bedded micritic deposits (Fig. 5) with tepee structures and mudcracks indicate shallow water precipitation of magnesite with emergent evaporative conditions. A marine coastal environment is interpreted from evidence of tidal effects observed in the bimodality of ripple cross-lamination data in sandy interbeds and distinct change in the direction of imbrication within individual clast-dominated conglomerate beds, indicating the presence of reversing currents (Frank and Fielding 2003). The interpretation is supported by isotope data for magnesite where enriched ^{13}C and marginally enriched ^{18}O, relative to coeval dolomite, is consistent with isotopic evolution of seawater during evaporation (Belperio 1990; Frank and Fielding 2003). Also, boron content in magnesite is high, at between 40–250 ppm B (Horn et al. 1999). By comparison, magnesites hosted in continental fluvial/lacustrine deposits at Kunwawara contain <10 ppm B (Burban 1990).

Magnesite conglomerates were deposited with both normal and inverse grading indicating deposition from turbulent flows with high solids content. There is, however, little evidence for storm wave activity, i.e. no hummocky cross-stratification. The formation of repetitive interbeds of intraclastic magnesite was most likely the result of periodic sheetflooding caused by inland rain events. Floodwaters that spread across extensive low-gradient tidal flats disrupted and reworked semi-lithified magnesite crusts into high-concentration mud flows with the entrained solids redeposited in shallow water as conglomerate to be reworked by tidal currents (Frank and Fielding 2003). These mostly thin beds were extensively distributed along the coast for tens of kilometres and seaward for over 2 km, where these can be traced across the Witchelina syncline (Horn et al. 1999). The clastic magnesites were later infilled and cemented by fine-grained carbonate mud of magnesitic or dolomitic composition and then covered by dolomitic mudstone, commonly with stromatolite biostromes. At times, the abundance of tabular stromatolite biostromes so dominated the coastal environment that distinctive marker beds of dark grey micritic dolomite with black chert nodules formed that are resistant to weathering and have unique characteristics such that individual beds can be confidently traced along strike for more than 12 km (Uphill 1990).

Extensive deposits of marine sedimentary magnesite are rare in the geological record, even during the Proterozoic period when marine dolomite was widespread. Paleoproterozoic marine magnesites have been described from the NW Fennoscandian Shield in Russia (Melezhik et al. 2000). These include 1–15 m thick beds of sedimentary micritic and stromatolitic magnesite. The lateral extent of the deposits is unknown, but they formed as shallow marine deposits under evaporitic conditions, possibly with periodic dilution from meteoric groundwater inflows. The finely laminated micritic magnesite facies is comparable to micritic magnesite of Skillogalee Dolomite, but other facies differ in that they show evidence of gypsum crystallisation and early diagenetic replacement of fine-grained dolomite by micritic magnesite. Patches of coarsely crystalline magnesite are also present as the result of partial recrystallisation of micritic magnesite during greenschist metamorphic conditions. Intraformational magnesite conglomerates are

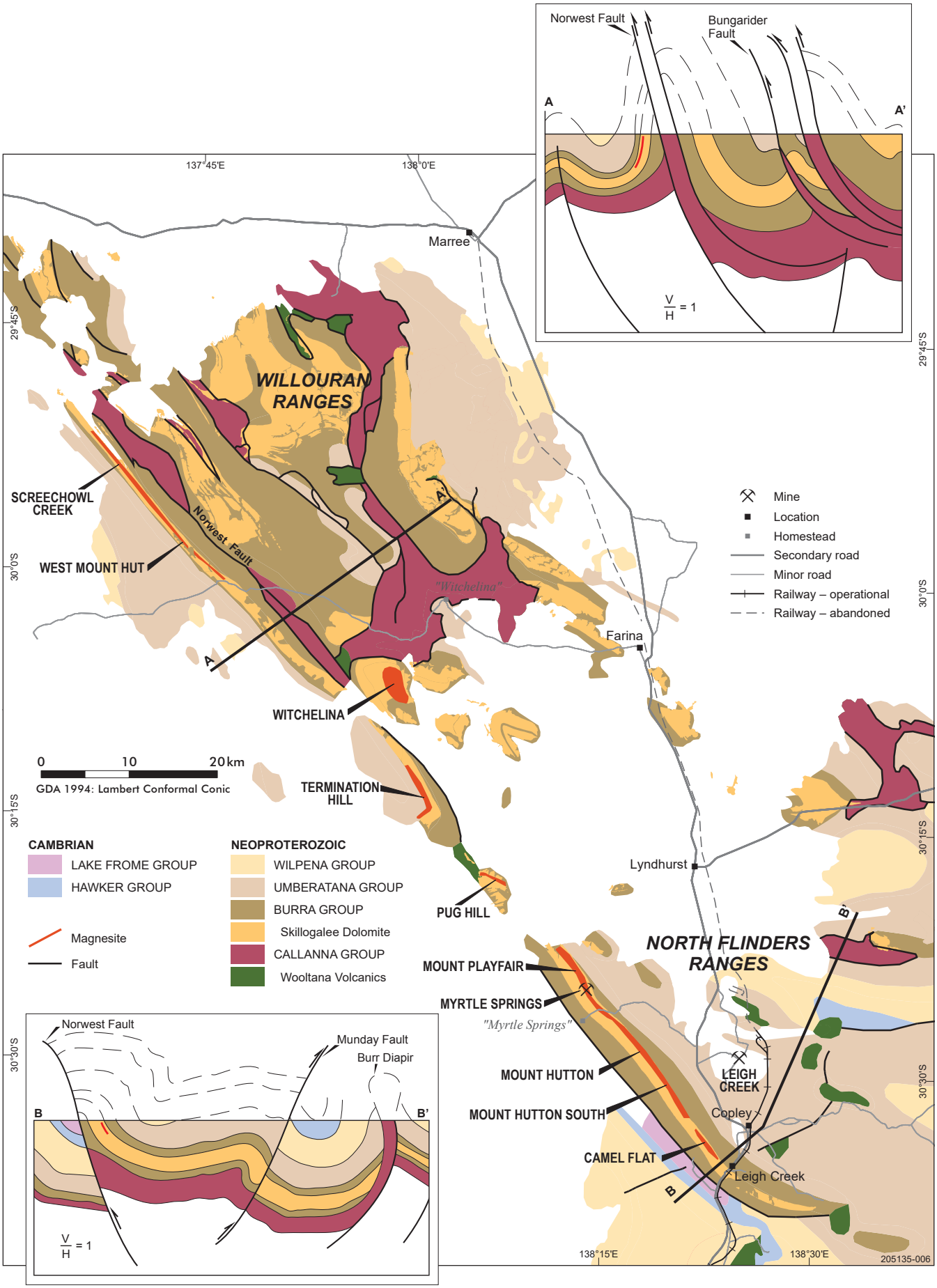

Figure 3 *Geology and location of sedimentary magnesite deposits and prospects in the northern Flinders and Willouran ranges. Geological cross-sections modified from Mackay (2011; A–A'), and Paul, Flöttmann and Sandiford (1999; B–B').*

Figure 4 *Magnesite pebble conglomerate (width 0.55 m) with thin grey dolomite interbeds (10–40 mm thick), Screechowl Creek. (Photo 046340)*

Figure 5 *Finely bedded micritic magnesite, 0.7 m thick, showing tepee-like structures in the lower bed, Screechowl Creek. (Photo 046341).*

absent. Other large magnesite deposits hosted by Proterozoic carbonate rocks occasionally show sedimentary structures indicative of evaporative marine environments (e.g. Dong et al. 2016), but the large size of the deposits is invariably the result of later metasomatic fluid infiltration, leading to wholesale dolomite replacement and magnesite recrystallisation.

Conditions necessary to form extensive deposits of primary magnesite by direct precipitation from seawater were possibly restricted to the Neoproterozoic during a period of sustained high Mg/Ca (>10) oceans from c. 790 Ma (late Tonian) to c. 670 Ma (mid-Cryogenian) (Hood and Wallace 2018). High content of sulfate in present day oceans inhibits dolomite precipitation, but Proterozoic oceans were sulfate poor and dolomite formed by direct precipitation (Shen, Cranfield and Knoll 2002). Even under these circumstances, evaporative concentration of seawater would normally precipitate $CaSO_4$ minerals together with any magnesite. The rarity of $CaSO_4$ minerals in Skillogalee Dolomite magnesite deposits is regarded by Frank and Fielding (2003) as an important indicator of the change in ocean chemistry at c. 790 Ma, where high Mg/Ca, low sulfate and $HCO_3^-/Ca^{2+}>2$ combined to maximise dolomite precipitation. In shallow evaporative coastal marine environments with active algal communities, high dolomite production effectively removed seawater calcium, allowing excess magnesium to further concentrate and precipitate magnesite without coprecipitation of $CaSO_4$ minerals. These conditions appear to have prevailed across widespread peritidal mudflats along the northwestern margin of the marine Adelaide Geosyncline. In this emergent peritidal environment, however, preservation of thin magnesite deposits was not assured. Rather, the repetitive events of partial induration, erosion and redeposition into shallow seawater with subsequent burial by marine dolomitic mud were important processes in preservation of the extensive peritidal, primary magnesite deposits.

Following deposition of Skillogalee Dolomite, subsidence continued through reactivated rifting along the western margin of the geosyncline, followed by periods of 'thermal sag' (Jenkins 1999). The subsidence accommodated a further 6,000–8,000 m of sediment on top of Burra Group, east of the Norwest Fault, as estimated from a reconstructed section near Copley (Paul, Flöttmann and Sandiford 1999). At maximum depth of burial, the temperature of upper Burra Group sediments is estimated at between 150–240 °C, assuming conservative thermal gradients for sedimentary basins of 25–30 °C km^{-1}. Depth of burial and temperature equate with very low-grade metamorphic conditions, extending into lower greenschist facies. The conditions were not sufficiently high to recrystallise micritic magnesite and dolomite, but diagenetic changes are present that include the growth of small euhedral albite crystals and development of stylolites of dolomite and magnesite composition. Also, talc formed as fine flakes, in part replacing dolomite cement along the margins of magnesite clasts, and occasionally as finely disseminated flakes, randomly orientated, within magnesite clasts (Fig. 6). The presence of low temperature talc is unusual, but has been reported previously in Neoproterozoic stromatolitic carbonates from Yukon, Canada, where talc formed during early diagenesis of platform carbonates, under chemical conditions that were possibly mediated by microbial activity (Tosca et al. 2011). Talc in Skillogalee Dolomite magnesites appears to have formed during latter stages of compaction, most probably via reactions involving silica-rich pore fluids. Experiments by Wan et al. (2017) demonstrated that silica fluids will react with dolomite to form talc at <200 °C, provided aluminium content is low and evolved CO_2 product is free to diffuse.

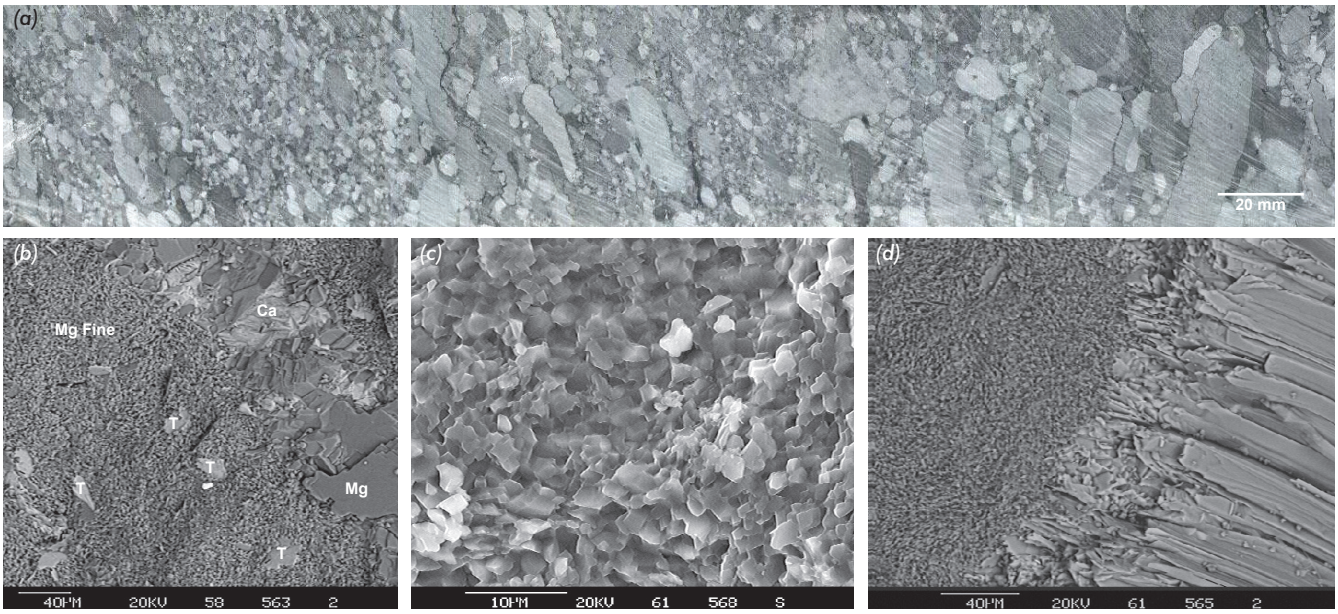

Figure 6 *Magnesite textures and mineralogy.* ***(a)*** *Drill core through magnesite pebble/cobble conglomeration at Mount Hutton (MHDD55, 51.3–51.6 m).* ***(b)*** *Cryptocrystalline magnesite (Myrtle Springs) with minor talc (T) flakes and stylolite vein of coarse crystalline magnesite (Mg) and calcite (Ca) (upper right).* ***(c)*** *Detail of cryptocrystalline magnesite clast showing porosity and 2–5 µm crystal size.* ***(d)*** *Cryptocrystalline magnesite clast (left) with overgrowth of radiating talc crystals (Witchelina deposit). (Photos 417747–417750)*

Sedimentation in the Adelaide Geosyncline ceased in the Early Cambrian with regional compression leading to basin inversion during the Delamerian Orogeny (c. 510–490 Ma). Along the western margin of the northern Flinders Ranges, upright kilometre-scale open folds were formed about NW–SE fold axes creating long limbs with moderate to steep dips. Strain developed during basin shortening, of ~20% in a NE–SW direction, is not reflected in increase in metamorphic grade nor mineral recrystallisation, but rather was taken up largely in the reversal of movement on earlier faults forming the rift margin, particularly the Norwest Fault (Paul, Flöttmann and Sandiford 1999). Minor faults developed also that trend mostly N–S to NNW–SSE. These displace sections of magnesite beds by <1–15 m, with occasional larger faults displacing thick dolomite–magnesite sequences by >25 m (McCallum 1986; Horn 2004a). Despite this, many areas of regular stacked sequences of magnesite and dolomite of consistent thickness can be traced along strike for several hundred metres without obvious fault offset. Quartz content as detrital grains in magnesite is typically <0.5%, and vein quartz is rare, except in areas of structural deformation.

Magnesite resources and evaluation

Recent interest in further development of South Australian magnesite resources has focused on Neoproterozoic sedimentary magnesite along the western margin of the northern Flinders Ranges. Magnesite deposits are known from other districts and some have recorded production (Crettenden 1985). These include metasomatic replacement-style 'sparry' magnesite at Balcanoona in Neoproterozoic dolomitic carbonate, interbedded sedimentary magnesite in Skillogalee Dolomite, east of Port Germain, surficial replacement of dolomite by magnesite near Robertsown in the Mid North, and modern playa lake deposits of dolomitic magnesite near Meningie in the Coorong district of the South East (von der Borch and Lock 1979; Crettenden 1985). The most extensive magnesite deposits, however, are distributed in the northern Flinders Ranges as interbeds in Skillogalee Dolomite. These are thickest and most abundant in the belt of folded rocks that extends NW from Leigh Creek, in the south, to a point ~2.5 km NW of Screechowl Creek on the southwestern flank of the Willouran Ranges (Fig. 3). Over a distance of 105 km, 10 individual magnesite deposits/prospects have been outlined with combined resources of >500 Mt at >40% MgO (Table 2). This represents one of the world's largest known resources of cryptocrystalline magnesite.

Thin beds of mostly magnesite conglomerate vary in thickness from a few centimetres to 10 m and are concentrated in the upper half of Skillogalee Dolomite. Magnesite clasts composed of cryptocrystalline fragments 1 to 100 mm in size vary from platy to rolled 'ripped-up' mud layers, to rounded pebbles grading to magnesite sand, all in a matrix of microcrystalline dolomite or magnesite. The degree of sorting and grain size can vary markedly between beds, but the characteristics of individual beds tend to be consistent.

Table 2 *Magnesite resource estimates, northern Flinders Ranges and Willouran Ranges*

Deposit	Measured (Mt)	Indicated (Mt)	Inferred (Mt)	Total (Mt)	MgO* (%)
Camel Flat	Nil	5	8	13	42.0
Mount Hutton South	Nil	10	20	30	42.9
Mount Hutton	18.3	42	53	113.3	42.9
Myrtle Springs	1	5	5	11	42.9
Mount Playfair	Nil	16	28	42	42.5
Pug Hill	Nil	10	10	20	42.7
Termination Hill	4	5	20	29	42.8
Witchelina	23.7	94	99	216.7	40.0
West Mount Hut	Nil	Nil	67	67	44.3
Screechowl Creek	Nil	Nil	36	36	44.3
Total	**47**	**187**	**346**	**578**	**42.0**

* MgO content includes contribution from dolomite and talc (source: Horn, Keeling and Olliver 2017).

At the Camel Flat deposit bedding dips at 70° NE and more than 60 individual beds of magnesite, of maximum thickness 3 m, were reported in crosscutting sections exposed along Scammel Creek and Camel Flat Creek (McCallum 1986). Individual beds vary in the relative proportion of magnesite clasts to dolomitic matrix, but most show consistent grade along strike. Dolomites interbedded with magnesite tend to be thicker and while the contact with overlying magnesite is usually sharp, the top of magnesite beds with overlying dolomite can be more gradational. Magnesite beds tend to weather white, and at the surface are distinctive from pale grey to dark grey interbedded carbonaceous dolomite; the colour distinction reduces with depth.

The regular and predictable distribution of magnesite and dolomite interbeds and their similarity in physical properties dictates that selective mining of individual magnesite beds is preferred to bulk mining with subsequent separation of magnesite from dolomite by metallurgical approaches. An effective mining technique was developed by David Linke Contracting Pty Ltd for operations at the Myrtle Springs quarry where overlying dolomite, dipping ~60° NE, is removed to expose a clean top of magnesite bed making the full height of the benched quarry face (Fig. 7).

Figure 7 *Myrtle Springs quarry in interbedded dolomite (grey-pale brown) and magnesite (white); magnesite bed 5 cleaned and ready for precision blasting and extraction in 1998. (Photo 046337)*

Small explosive charges placed in shot holes drilled along the basal contact and at the toe of the magnesite bed are used to break the magnesite and encourage clean parting along the sharp contact with underlying dolomite. Broken ore is extracted from the toe of the face and the magnesite above is dropped to the quarry floor with the aid of a hydraulic rock pick which is used also to break up larger fragments. Staggered quarry faces, along strike, permit the mining of several individual magnesite beds, which can then be blended during crushing and stockpiling to maintain a consistent product. Some minor upgrading of magnesite is achieved by screening the crusher product and rejecting the fine material, which is higher in dolomite and talc matrix component. Trials to further upgrade raw magnesite by flotation and heavy media separation were unsuccessful due to the very fine grain size and intimate mix of the contaminant phases, principally dolomite and talc, which bond strongly with the magnesite clasts (Horn 2004b). Also, there was only a small difference in average specific gravity of magnesite (2.95) and dolomite (2.86) (Mount Hutton data; Horn et al. 1999). Cryptocrystalline magnesite clasts contain minor to trace amounts of Ca, Si and B, which reflect the alkaline marine conditions of formation (Keeling, McClure and Raven 1998; Keeling, McClure and Beech 1999).

Early exploitation of magnesite resources at Camel Flat and Witchelina selectively removed sections of outcropping magnesite beds to produce magnesium chemicals, mostly hydrated magnesium sulfate (Epsom salts) for the pharmaceutical industry. Some magnesite was used for magnesium metal manufacture during the Second World War. Product from Myrtle Springs quarry was sold as a flux coating for welding electrodes and later for fertiliser, as an additive in animal feed, and for trial CCM production for filtration of treatment water in aluminium smelting (Crettenden 1985). The presence of micritic dolomite and talc, which are not easily removed, and the high boron content, downgraded the potential for use in basic refractories, particularly for high-quality

DBM and EFM, which require very low levels of impurities. Some consideration was given to an approach involving dissolving the ore with SO_2 to extract magnesium as magnesium sulfite hydrate, which could be calcined to give high purity MgO (Commercial Minerals Ltd 1992).

In the mid-1990s, anticipated increased demand for magnesium metal as a primary component in lightweight metal alloys for the automobile industry, to reduce vehicle weight and lower fuel consumption, prompted a reappraisal of magnesite resources in South Australia. The South Australian magnesium metal initiative was commenced by the state government in 1996 and subsequently taken on by PIMA Mining Ltd (later Magnesium International Ltd). The Geological Survey was tasked with determining the extent of the resource and investigating geological factors affecting magnesite quality. Bulk sampling was done for preliminary test work, through Australian Mineral Laboratories (Amdel) Ltd, under the guidance of consultants Hatch Ltd, to produce magnesium chloride salt for electrolytic magnesium metal manufacture. Preliminary results were encouraging in that resources with consistent grade were confirmed to be large, and cryptocrystalline magnesite was highly reactive and readily dissolved in acid. Talc, feldspar and free quartz impurities were insoluble in acid, and calcium from dolomite could be selectively removed as insoluble sulfate. The project trialled new airborne hyperspectral techniques to effectively identify continuity of magnesite-bearing sequences and to locate stratigraphic horizons where magnesite beds were concentrated (Keeling and Mauger 1998; Keeling and Mauger 2000). This was followed up with on-ground mapping of marker beds and measurement of magnesite interbed thickness in surface exposures at prospects Screechowl Creek, Termination Hill and Mount Hutton (Horn et al. 1999). Representative bulk samples were collected for chemical and mineralogical analyses (Keeling, McClure and Raven 1998).

The approach was continued by PIMA Mining and extended through a program of diamond core drilling on five prospects (Pug Hill, Mount Hutton, Termination Hill, Myrtle Springs, Witchelina) to evaluate continuity of surface data and determine the size and grade of resources (Horn 2000). This work underpins much of the resource estimates summarised in Table 2. PIMA Mining identified Mount Hutton and Witchelina as key sites for development. Additional resource drilling was completed during 1999 at Mount Hutton, culminating with a mineral lease application, mine plan, and excavation of a trial pit slot to extract representative bulk samples. Ultimately the project to build a magnesium smelter in South Australia was abandoned in 2004 when growth in magnesium metal demand failed to achieve projected levels and increase in the cost of electricity favoured small-scale carbothermal manufacture of magnesium metal out of China, using local high-grade dolomite and magnesite feedstock.

The experience of mining at the Myrtle Springs quarry influenced the approach in defining and evaluating similar magnesite resources. Sites with moderate to steeply dipping beds required comparatively close-spaced magnesite beds of mineable thickness and grade. Thin magnesite interbeds within upper Skillogalee Dolomite can persist throughout ~800 m of stratigraphic thickness, but prospects and deposits mostly occupy a single stratigraphic interval where maximum tonnage might be extracted under practical constraints of waste to ore ratio <7:1 for magnesite interbeds >0.4 m thickness and grade >40% acid-soluble MgO. While such intervals may be traced along strike for tens of kilometres, the total thickness of a sequence comprising closely spaced magnesite interbeds rarely exceeds 100 m. At the Mount Hutton prospect, bedding dips 60–68°NE and reconnaissance drilling across the prospective upper section of Skillogalee Dolomite intersected up to 86 interbedded magnesite and dolomite units (Horn, Keeling and Olliver 2017). Resource estimates were confined to a 55 m thick central stratigraphic zone where 18 of 22 magnesite interbeds met thickness and grade specifications giving a composite thickness of 15.5 m of magnesite grading >40% MgO (HCl acid-soluble basis). This interval is broadly equivalent to that of the Camel Flat deposit in the SE, extending through Myrtle Springs to Mount Playfair in the NW, a total distance of ~25 km. Resources at Mount Hutton were calculated to 60 m vertical depth. Proposed mine development during 1999–2001 included additional drilling to upgrade the resource category over 4.7 km strike length, termed the Mount Hutton Central magnesite deposit. A measured resource was calculated for an

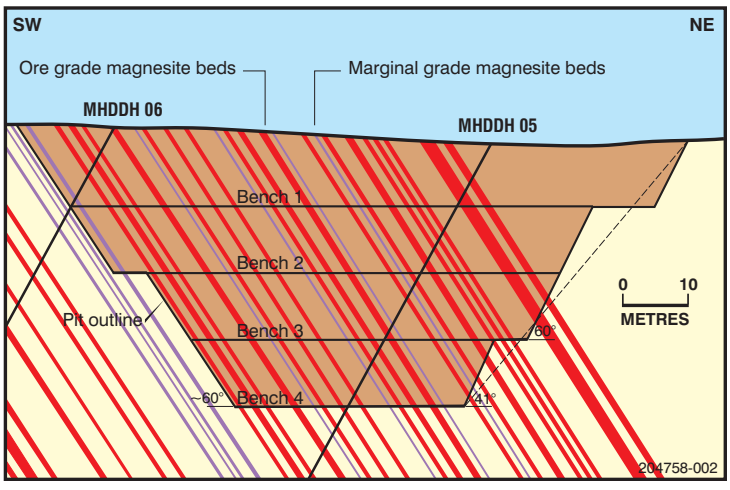

Figure 8 *Mount Hutton – optimised mine development section for extraction of 18 magnesite beds.*

optimised pit design of four 10 m benches (Fig. 8). The calculations were reviewed in 2016 by Archer Exploration Limited to comply with JORC 2012 (Joint Ore Reserves Committee), confirming extractable resources at Mount Hutton Central of 17.5 Mt at 40.1% MgO (Archer Exploration 2016), within the broader Mount Hutton resource. Specific gravity of magnesite beds varies from 2.90 to 3.03.

Mineable thicknesses of magnesite in the remote Screechowl Creek prospect in the Willouran Ranges were identified from field mapping and measured sections as continuous over 6.5 km. A steeply dipping (65–85° SW) package of 18 magnesite beds, ranging in thickness from 0.7 to 3.9 m, gave 33 m aggregated thickness of magnesite, interbedded with dolomite, across 95 m width. Airborne spectral mapping confirmed this interval of Skillogalee Dolomite contained the highest concentration of persistent magnesite interbeds in the more prospective southwestern area of Willouran Ranges (Keeling and Mauger 1998). Representative surface samples were collected and analysed but the site was not drill tested. An inferred resource of 36 Mt at 44.3% MgO (total extraction) to 60 m vertical depth was based on surface mapping and field sampling and the assumption that physical and chemical characteristics would persist down dip, as recorded in drilled deposits further to the south. Airborne spectral data was interpreted to extend the deposit a further 22 km SE to West Mount Hut, with additional inferred resources, assuming comparable thickness and grade recorded for magnesite mapped at Screechowl Creek (Horn et al. 1999).

Witchelina magnesite prospect differs from other magnesite prospects in the district in that it occupies the central zone of an open synclinal basin. Resource estimates were variously compiled across an area ~5 by 2 km, elongated NNW–SSE, which included magnesite beds throughout ~700 m of stratigraphic thickness (Fig. 9). The areal extent, predictable structure, sites with shallow dip, and the presence of individual thick magnesite interbeds, e.g. Bed 4 averages 8 m thickness, offer flexibility in mine development and a substantially larger indicated resource to 100 m depth (Table 2). Magnesite grades are lower (40% MgO total extraction) due to higher dolomite content, mostly as intraclastic cement infilling between magnesite clasts, which are generally less coarse and better sorted than at other prospects. Dolomite interbeds are thicker but waste to ore ratios are comparable with other deposits due to higher average thickness of magnesite interbeds at 1.5–2.0 m. Total magnesite resources in the Witchelina syncline of 215 Mt at 40% MgO are nearly twice that of the Mount Hutton deposit, the next largest resource in the district.

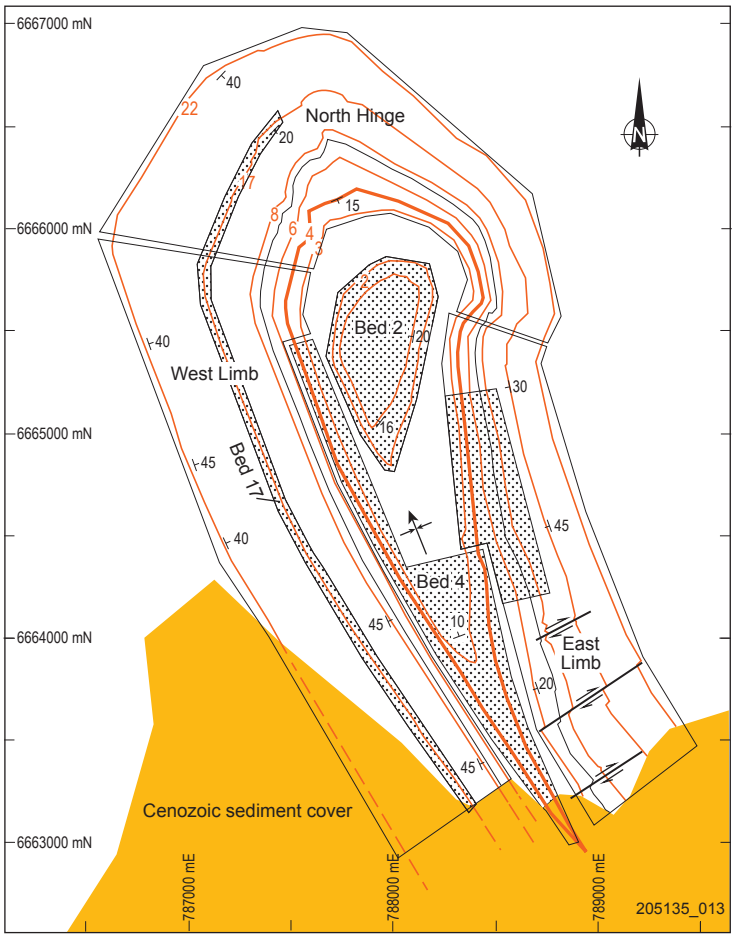

Figure 9 *Witchelina syncline, showing trace of magnesite beds (red) and outline of areas for resource calculation. (From Horn et al. 1999; GDA94 map coordinates)*

Despite the very large resources, the presence of fine-grained impurities and the requirement for selective mining of narrow magnesite beds have constrained development, especially for high-grade markets where beneficiation by dissolution would not be cost competitive. Opportunity for further development of the resources followed successful trials during development of the Calix Flash Calciner, leading to acquisition of the Myrtle Springs mine by Calix in 2012.

Development of the Calix kiln technology

Multiple hearth furnaces are widely preferred to produce CCM. This is a vertical calciner consisting of a stack of circular hearths where magnesite is fed from the top and is moved over the surface of each hearth by the action of rotating arms. Oxidising gases are fed from below and the temperature increased to 900–1,000 °C as the magnesite moves down over successive hearths to emerge at the bottom as calcined MgO. The rate of raw feed

charge, temperature and residence time on each hearth, and rate of rotation are varied to achieve a product with desired final properties.

The design of a new approach to calcination was a response to calls to reduce or eliminate CO_2 pollution through efficient carbon capture in the fossil fuels industry. The removal of carbon and a move to hydrogen energy would permit the use of fossil fuels without generating uncontrolled CO_2 waste. Alternatively, CO_2 could be captured directly from power plant flue gas streams. Calcium-looping is a technique where CaO is reacted with gaseous hydrocarbons or exhaust flue gas to remove carbon/CO_2 to give $CaCO_3$ (Ball and Sceats 2010). The calcium oxide sorbent is then regenerated by calcination of $CaCO_3$ under conditions where pure 'chemical-grade' CO_2 can be captured for other industrial uses or condensed and compressed for transport and disposal. Regenerated CaO would be recycled, potentially many thousand times. The process is thermodynamically efficient in that reaction to form $CaCO_3$ is exothermic while desorption of CO_2 is endothermic and if effectively coupled through a heat transfer or 'Endex' process could operate at low cost (Ball 2014). The challenge to reduce the operating temperature of the endothermic reaction to more closely match that of the exothermic reaction (~650 °C) and to produce a highly reactive CaO product whilst also capturing all the evolved CO_2 led to an innovative kiln design by retired Queensland mining engineer Connor Horley in collaboration with Mark Sceats (then at the University of Sydney). While the economics of calcium-looping technology for CO_2 capture in the fossil fuels industry continue to be evaluated (e.g. Perejón et al. 2016) it was clear that the new kiln design had wider application to other industries producing calcined carbonate minerals, including CCM, lime and cement industries. The concept and plant design were described in United States patent application in 2007, which was granted in 2014, assigned to Calix, a private company founded in 2005 by Sceats and Horley (Sceats, Horley and Richardson 2007). The first batch pilot test plant was built in 2007 at Jacobs Creek, Queensland, with a continuous process plant built in 2010 at Bacchus Marsh, Victoria, followed by commissioning in 2013 of a commercial-scale demonstrator plant (Fig. 10) with operating capacity 25,000 tpa MgO (Calix 2018). Testing of various carbonate raw materials, including magnesite from the Myrtle Springs mine, showed cryptocrystalline magnesite could be calcined in the kiln at the comparatively low temperature of ~760 °C to give a superior, highly reactive MgO product offering some commercial

Figure 10 *Calix Flash Calciner – commercial-scale demonstrator plant at Bacchus Marsh in 2013, and diagram of key components of the kiln system. (Courtesy of Calix; photo 417751).*

advantage. Calix acquired the Myrtle Springs quarry in 2012 as a long-term source of magnesite for the Bacchus Marsh plant (Calix 2018).

The Calix flash kiln technology uses a vertical reactor where finely ground raw feed is input at the top along with the injection of superheated steam (Fig. 10). The granular mix of particles and gas moves rapidly through an enclosed helix reactor tube where the rate and turbulence of flow are modified by the force of steam injection, in combination with gravitational and centrifugal forces. The reaction tube is heated externally with heat transferred through the wall of the tube to affect the calcination, aided by catalytic action of the steam. Maximum temperature in the tube is achieved at the point of exhaust. Calcined particles are produced with very short (<10 seconds) residence time in the reaction chamber to give a high surface area product with >95% calcined particles (Sceats, Horley and Richardson 2007). Evolved CO_2 gas is extracted with the steam at a gas-granule separator using reversing axial separator technology where the flow direction is reversed at the bottom of the reactor (LEILAC 2016). The gas and steam travel up an internal tube and exit the reactor where the gas is filtered to remove any entrained fine solids. The calcined solids exit from the bottom of the reactor. Steam is condensed and recycled back to the reactor and evolved CO_2 is captured and stored separately.

Key attributes of the Calix Flash Calciner include:

- Short residence time of 1–10 seconds in the calciner reactor is several orders of magnitude shorter than for conventional kilns, which allows for a much smaller volume and weight of kiln to produce the same output of calcined product.
- Use of steam to catalyse the reaction – where steam under high partial pressure adsorbs on the surface of magnesite and acts to weaken the bonding of CO_2 to Mg, such that when calcination temperature is approached the reaction rate is reduced to seconds.
- Use of pre-ground feedstock with particle size range selected to give the required high surface area for maximum calcination – typically in the range 40–250 μm.
- The speed of calcination reaction allows for greater temperature control, which together with the short residence time restrict the opportunity for sintering reactions that reduce surface area through partial melting and agglomeration of granules.
- Arrangement of the helix reactor tube limits the acceleration of the granules through the reactor as CO_2 is evolved and provides a high surface area for heat transfer while maintaining a compact reactor system.
- The centrifugal force imparted to the granules in the flow ensures that the granules are in close contact with the tube wall for maximum heat transfer.
- Interaction of the particles with the tube wall and with the turbulent flow of entraining steam/gas induces a pressure drop through the reactor that is sufficiently low at the exit point as to limit the partial pressure of CO_2 and therefore suppress the effect of back reaction (i.e. recombination of MgO and CO_2).
- All CO_2 generated from the calcination reaction is separated and captured within the closed system.

Cryptocrystalline magnesite from Myrtle Springs is delivered to the Bacchus Marsh plant as <40 mm screened aggregate. This is ground to <0.25 mm for feed to the Calix Flash Calciner. Calcined MgO product is highly reactive CCM with specific surface area >100 m^2/gm (BET, Brunauer–Emmett–Teller) but kiln conditions can be adjusted to produce CCM product with specific surface area approaching 300 m^2/gm (BET). This compares with more typical specific surface areas of 20–40 m^2/gm for lightly calcined MgO (Shand 2006). Macrocrystalline magnesite tends to crack and break into fragments as CO_2 is evolved during calcination without creating a large increase in surface area (Ozdemir 2012). Cryptocrystalline magnesite with inherent porosity permits loss of CO_2 from fine particles with much less fragmentation. This substantially increases the porosity and surface area of the particle. The effect is enhanced in the presence of super-heated steam at low calcination temperature and is most effective in creating high surface area in the compact, low-grade metamorphosed cryptocrystalline magnesite from the northern Flinders Ranges.

Market developments and opportunities for cryptocrystalline magnesite

The combination of new kiln technology and suitable magnesite resource that deliver a high surface area, highly reactive magnesia product from cryptocrystalline magnesite creates an opportunity to expand CCM markets. Calix has been active in developing these opportunities, while furthering the application of their kiln technology in allied industries, including cement and lime manufacture. Developments in CCM markets include water treatment and infrastructure protection; aquaculture; agriculture; and building materials.

Water treatment and infrastructure protection

$Mg(OH)_2$ slurry made from CCM mixed with up to 50% water by weight is used to neutralise acidic

wastewater and treat sewage waste to maintain pH and control odour from H_2S generated by anaerobic bacteria activity at pH <7. In this market, $Mg(OH)_2$ competes with lime (CaO), caustic soda (NaOH), ferric chloride ($FeCl_3$) and calcium nitrate ($Ca(NO_3)_2$). The high reactivity of MgO product from calcination of cryptocrystalline magnesite in the Calix Flash Calciner offered cost savings in $Mg(OH)_2$ liquid makeup that contributed to early commercialisation. In Australia, $Mg(OH)_2$ liquid is traditionally made by wet-grinding MgO with an equal volume of pre-heated water. Highly reactive MgO can make $Mg(OH)_2$ liquid by shear mixing in water at ambient temperature. A smaller scale mixing plant is required that can be set up near the site to be treated, thereby reducing plant capital costs and lowering transport costs. Reduced delivered cost, combined with other advantages of $Mg(OH)_2$ liquid in terms of ease of handling, low environmental impact, and extended performance in maintaining pH, has improved competitiveness and access to markets that were previously cost prohibitive (Calix 2018).

Release of H_2S in sewer systems creates additional problems through concrete corrosion due to conversion of H_2S to sulfuric acid by bacterial action and oxidation. The life of aging concrete sewer assets can be extended by high-pressure water cleaning and then coating with $Mg(OH)_2$ slurry, which raises the pH and eliminates the bacteria responsible for sulfuric acid production (Apté 2015). The use of $Mg(OH)_2$ mixed with additives to facilitate spray application and rapid gelling on concrete surfaces has been applied successfully by Calix in trials to protect sewer lines and manhole access, leading to uptake by municipal bodies, including councils in Queensland and the Sydney Water Corporation (Calix 2018).

Aquaculture

In aquaculture the addition of high surface area $Mg(OH)_2$ with some added calcium carbonate has been effective in improving water quality and pond bottom conditions. The effect is reduced turbidity, precipitation of iron and other heavy metals, reduced hydrogen sulfide with stabilised seawater alkaline pH, along with reduced sludge and increase in phytoplankton production. Successful trails by Calix in commercial aquaculture in the Philippines and Thailand have improved water quality and pond bottom conditions resulting in increased health and productivity of shrimp and fish. Trials were recently extended to aquaculture operations in northern China to investigate approaches to control nitrite levels in sludge produced during intensive shrimp farming (Calix 2017).

Agriculture

Demand for more environmentally friendly fungicides and pesticides has seen renewed interest in mineral-based sprays as safer and more affordable alternatives. Trials in Australia using high surface area $Mg(OH)_2$ as a foliar spray showed success with reducing pest and disease pressure in tomato, banana, pineapple, cassava and grape plantings with corresponding improvement in crop vitality and yield (Calix 2015b). The effect is attributed in part to the high surface area of the $Mg(OH)_2$ particles which have high porosity and internal/external crystal faces of nano-sized dimensions. Charge imbalance on edge-sites and corners of nano-surfaces and an alkaline environment appear to stabilise reactive oxygen species (ROS), which can then interact with and deactivate bacterial and fungal pathogens in much the same way as the plant's production of ROS acts as a natural defence to pathogen infection (Sceats and Hodgson 2018; Calix 2015a). $Mg(OH)_2$ particles at pH 10.4 also neutralise acids exuded by pathogens, and the release of Mg and OH ions may also play a role in antibacterial mechanisms (Pan et al. 2013). While the $Mg(OH)_2$ derived from cryptocrystalline magnesite show nanoparticle activity they remain durable particles, 10–100 μm in size, and therefore do not pose the same handling concerns as nano-sized particles, which are breathable and can diffuse through the skin. In practical use, the ultimate breakdown of $Mg(OH)_2$ particles provides Mg, which is an essential plant nutrient.

Building materials

Magnesia-based cements have a history of technology development over 150 years with specialist uses primarily in industrial flooring and insulating panels where they contribute soundproofing, dust-free, low thermal conductivity and fire-retardant properties. Magnesium oxychloride (Sorel) cement is most widely used and is made by mixing magnesia with magnesium chloride solution, but other cement systems include magnesium oxysulfate and magnesium phosphate (Shand 2006). Drawbacks with Sorel cement include cost, water-soluble phases that limit use to areas not exposed to prolonged wetting, and incompatibility with steel reinforcing due to corrosion by leached magnesium chloride salts (Walling and Provis 2016). Despite the limitations, magnesia-based cements are preferred for some applications and are more environmentally friendly due to lower CO_2 emissions than that for Portland cement (PC) production. The addition of reactive magnesia to PC has advantages in large-scale civil engineering projects where expansion during formation of $Mg(OH)_2$ can compensate for natural shrinkage over time

and improve strength when large volumes of PC are used (Du 2005). The use of larger additions of reactive magnesia to PC and the use of CO_2 during curing to form carbonate minerals as a means of sequestering CO_2 in the manufacture of building products are subjects of ongoing investigations (Walling and Provis 2016). Research in this area by Imperial College of London led to a patented process, Novacem technology, which was acquired by Calix in 2012 and provides the basis for their trial manufacture of MgO blocks, tiles and wall boards that effectively remove atmospheric CO_2 during curing.

Conclusion

The Australian invention of the Calix kiln technology is an example of how innovation and application can deliver practical solutions to address the requirement to manage CO_2 emissions. For the industrial minerals sector concerned with the calcination of carbonate minerals such solutions may be essential to long-term viability. Importantly, the progress with the Calix kiln technology highlights how a change in approach can create opportunities to deliver solutions for other industries, leading to new markets.

For cryptocrystalline magnesites of the northern Flinders Ranges, the new kiln technology unlocks useful intrinsic properties of the raw magnesite, related to consistent fine particle size, porosity, and high degree of consolidation. The calcined product of durable MgO particles with high surface area and active nano-scale crystal surfaces provides superior properties for various existing and new uses. Growth in markets where high-activity MgO provides advantage, and where low levels of CaO and talc impurities are tolerated, appear set to underpin further development of South Australia's unique sedimentary magnesite resources.

Acknowledgements

The authors acknowledge the contribution of colleagues Anthony (Max) Pain, Peter Crettenden, Wolfgang Preiss (Geological Survey of South Australia), and Steve Biggins and Lindsay Owler (PIMA Mining) in mapping and sampling to define the extent of magnesite resources in the northern Flinders Ranges and western Willouran Ranges. Calix is thanked for permission to reproduce previously published Figure 10.

References

Apté N 2015. Know your sewer – corrosion protection of sewer assets. *Proceedings 9th WIOA, NSW Water Industry Operations Conference and Exhibition, Orange PCYC 24–26 March, 2015*, pp. 129–135.

Archer Exploration Limited 2016. *Mount Hutton Central JORC 2012 resource,* ASX release 12 April 2016. ASX, viewed 2 January 2019, <https://www.asx.com.au/asxpdf/20160412/pdf/436g9j7ltkjyq2.pdf>.

Ball R 2014. Entropy generation analyses of Endex and conventional calcium looping processes for CO_2 capture. *Fuel* 127:202–211.

Ball R and Sceats MG 2010. Separation of carbon dioxide from flue emissions using Endex principles. *Fuel* 89:2750–2759.

Belperio AP 1990. Palaeoenvironmental interpretation of the late Proterozoic Skillogalee Dolomite in the Willouran Ranges, South Australia. In JB Jago and PS Moore eds, *The evolution of a late-Precambrian-early Palaeozoic rift complex: the Adelaide Geosyncline,* Special Publication 18. Geological Society of Australia, pp. 85–104.

Burban B 1990. Kunwarara magnesite deposit. In FE Hughes ed., *Geology of the mineral deposits of Australia and Papua New Guinea*. The Australasian Institute of Mining and Metallurgy, Melbourne, pp. 1675–1677.

Calix Limited 2015a. *Oxide products formed from calcined carbonate powder for use as biocide, chemical detoxifier and catalysts support products*, International Publication Number WO 2015/100468 AI. International application published under the Patent Cooperation Treaty, World Intellectual Property Organization.

Calix Limited 2015b. Super-mag foliar spray for agriculture, *Calix News* 16. Calix, viewed 2 January 2019, <https://www.calix.com.au/news.html>.

Calix Limited 2017. AQUA-Cal+ for shrimp farming, *Calix News* 20. Calix, viewed 2 January 2019, <https://www.calix.com.au/news.html>.

Calix Limited 2018. *Calix Limited prospectus*, ASX release 19 July 2018. Calix, viewed 2 January 2019, <https://www.asx.com.au/asxpdf/20180719/pdf/43wmn3h1znxnsz.pdf>.

Chen C, Lu A, Cai K and Zhai Y 2002. Sedimentary characteristics of Mg-rich carbonate formations and minerogenic fluids of magnesite and talc occurrences in early Proterozoic in eastern Liaoning Province, China. *Science in China Series B: Chemistry* 45:84–92.

Commercial Minerals Ltd 1992. South Australian magnesium oxide project pre-feasibility study report, Open file Envelope 12065. Department for Energy and Mining, South Australia, Adelaide.

Crettenden PP 1985. *Magnesite in South Australia, a historical review 1915-1984*, Report Book 85/00062. Department of Mines and Energy, South Australia, Adelaide.

Department of Natural Resources and Mines, Queensland 2017. *Queensland's metalliferous and industrial minerals 2016*. Department of Natural Resources and Mines, Queensland, viewed 17 January 2019, <https://www.dnrm.qld.gov.au/__data/assets/pdf_file/0009/374859/metalliferous-industrial-minerals.pdf>.

Dong A, Zhu X-K, Li S-Z, Kendall B, Wang Y and Gao Z 2016. Genesis of a giant Paleoproterozic strat-bound magnesite deposit: constraints from Mg isotopes. *Precambrian Research* 281:673–683.

Du C 2005. A review of magnesium oxide in concrete. *Concrete International* 12:45–50.

Ebner F, Prochaska W, Troby J and Zadeh AMA 2004. Carbonate hosted sparry magnesite of the greywacke zone, Austria/eastern Alps. *Acta Petrologica Sinica* 20:791–802.

Flook R and Wilson I 2016. Chinese magnesia and refractories – the new normal. *Industrial Minerals* September 2016, pp. 48–55.

Frank TD and Fielding CR 2003. Marine origin for Precambrian, carbonate-hosted magnesite. *Geology* 31:1101–1104.

Hill BF 1992. The Queensland magnesia project: implementation of a major resource for the world refractory industry. In JB Griffiths ed., *Papers presented at the 10th Industrial Minerals International Congress*. Metal Bulletin, Surrey UK, pp. 75–81.

Hood AvS and Wallace M 2018. Neoproterozoic marine carbonates and their paleoceanographic significance. *Global and Planetary Change* 160:28–45.

Horn CM 2000. The South Australian magnesium metal project. *MESA Journal* 16:5–10. Primary Industries and Resources South Australia, Adelaide.

Horn CM 2004a. Exploration Licence 2565 - Partial surrender report for the period ending 18 November 2002, Open file Envelope 10529. Department for Energy and Mining, South Australia, Adelaide.

Horn CM 2004b. Exploration Licence 2565 - Final technical report for the period ending 18 November 2003, Open file Envelope 10529. Department for Energy and Mining, South Australia, Adelaide.

Horn CM, Keeling JL and Olliver JG 2017. Sedimentary magnesite deposits, Flinders Ranges. In GN Phillips ed., *Australian ore deposits*. The Australasian Institute of Mining and Metallurgy, Carlton, Victoria, pp. 671–672.

Horn CM, Owler L, Biggins S and Szmidel R 1999. Economic evaluation of magnesite deposits in the northern Flinders Ranges, Open file Envelope 09552. Department for Energy and Mining, South Australia, Adelaide.

Jenkins RFJ 1999. The Adelaide Fold Belt: tectonic reappraisal. In JB Jago and PS Moore eds, *The evolution of a late-Precambrian-early Palaeozoic rift complex: the Adelaide Geosyncline*, Special Publication 18. Geological Society of Australia, pp. 396–420.

Jiang S, Chen C, Chen Y, Jiang Y, Dai B and Ni P 2004. Geochemistry and genetic model for the giant magnesite deposits in eastern Liaoning Province, China. *Acta Petrologica Sinica* 20:765–772.

Jiang YH, Jiang SY, Zhao KD, Ni P, Ling HF and Liu DY 2005. SHRIMP U-Pb zircon dating for lamprophyre from Liaodong Peninsula: constraints on the initial time of Mesozoic lithosphere thinning beneath eastern China. *China Science Bulletin* 50:2612–2620.

Keeling J and Mauger A 1998. New airborne HyMap data aids assessment of magnesite resources. *MESA Journal* 11:7–11. Primary Industries and Resources South Australia, Adelaide.

Keeling JL and Mauger AJ 2000. Application of airborne hyperspectral (HyMap) data to map variation in carbonate facies in Proterozoic Skillogalee Dolomite, Willouran Ranges, South Australia. *Proceedings, 10th Australasian Remote Sensing and Photogrammetry Conference, Adelaide 21–25 August 2000*, pp. 923–930.

Keeling JL, McClure SG and Beech A 1999. *Boron in sedimentary magnesite from South Australia: results of scanning electron microscope investigation*, PIMA Mining Ltd [CSIRO Land and Water, Consultancy Report 99/44], Open file Envelope 09499. Department for Energy and Mining, South Australia, Adelaide.

Keeling JL, McClure SG and Raven MD 1998. *Mineralogy and chemistry of Proterozoic magnesite ores from South Australia* [CSIRO Land and Water Technical Report 7/98], Open file Envelope 09499. Department for Energy and Mining, South Australia, Adelaide.

Krupenin MT and Kol'tsov AB 2017. Geology, composition and physicochemical modelling of sparry magnesite deposits of the southern Urals. *Geology of Ore Deposits* 59:14–35.

LEILAC 2016. Public LEILAC pre-feed summary report. LEILAC, viewed 21 November 2018, <https://www.project-leilac.eu/publications>.

LEILAC 2017. Public LEILAC feed summary report. LEILAC, viewed 21 November 2018, <https://www.project-leilac.eu/publications>.

Mackay W 2011. Structure and sedimentology of the Curdimurka Subgroup, northern Adelaide Fold Belt, South Australia. PhD thesis, University of Tasmania.

McCallum W 1986. *Camel Flat magnesite deposit, near Copley, north western Flinders Ranges, Geological investigations, 1984 and 1985, MC 1836,1883 – David Linke Contractor* P/L, Report Book 86/00017. Department of Mines and Energy, South Australia, Adelaide.

Melezhik VA, Fallick AE, Medvedev PV and Makarikhin VV 2000. Palaeoproterozoic magnesite-stromatolite-dolostone 'red-bed' association, Russian Karelia: palaeoenvironmental constraints on the 2.0 Ga-positive carbon isotope shift. *Norsk Geologisk Tidsskrift* 80:163–186.

Milburn D and Wilcock S 1998. Kunwarara magnesite deposit. In DA Berkman and DH Mackenzie eds, *Geology of Australian and Papua New Guinean mineral deposits*. Australasian Institute of Mining and Metallurgy, Melbourne, pp. 815–818.

Mish D, Pluch H, Mali H, Ebner F and Hui H 2018. Genesis of giant early Proterozoic magnesite and related talc deposits in the Mafeng area, Liaoning Province, NE China. *Journal of Asian Earth Sciences* 160:1–12.

O'Driscoll M 2018. Basic instinct: magnesia supply to the refractories industry. *Refractories WorldForum* 10:1–4.

Olivier JGJ, Janssens-Maenhout G, Muntean M and Peters JAHW 2016. *Trends in global CO_2 emissions: 2016 report*. The Hague, PBL Publishers, Netherlands.

Ozdemir B 2012. *Cryptocrystalline and macrocrystalline magnesite ores*, Presentation MagMin Salzburg Austria 14–16 May 2012. Kümaş Manyezit Sanayi A.Ş., viewed 20 February 2019, <http://www.kumasref.com/en-EN/technical-publications-and-documents,KTE_424.html>.

Pan X, Wang Y, Chen Z, Pan D, Cheng Y, Lui Z and Guan X 2013. Investigation of antibacterial activity and related mechanism of a series of nano-$Mg(OH)_2$. *ACS Applied Material Interfaces* 5:1137–1142.

Parente CV, Ronchi LH, Sial AN, Guillou JJ, Arthaud MH, Fuzikawa K and Verissimo CUV 2004. Geology and geochemistry of Paleoproterozoic magnesite deposits (~1.8Ga), State of Ceara, northeastern Brazil. *Carbonates and Evaporites* 19:28–50.

Paul E, Flöttmann T and Sandiford M 1999. Structural geometry and controls on basement-involved deformation in the northern Flinders Ranges, Adelaide Fold Belt, South Australia. *Australian Journal of Earth Sciences* 46:343–354.

Perejón A, Romeo LM, Lara Y, Lisbona P, Martínez A and Valverde JM 2016. The calcium-looping technology for CO_2 capture: on the important roles of energy integration and sorbent behaviour. *Applied Energy* 162:787–807.

Perks C 2017. Life after steel: is there more for magnesia? *Industrial Minerals* April 2017, pp. 32–37.

Pohl W 1990. Genesis of magnesite deposits – models and trends. *Geologische Rundschau* 79:291–299.

Preiss WV 2000. The Adelaide Geosyncline of South Australia and its significance in Neoproterozoic continental reconstruction. *Precambrian Research* 100:21–63.

Preiss WV, Drexel JF and Reid AJ 2009. Definition and age of the Kooringa Member of the Skillogalee Dolomite: host for Neoproterozoic (c. 790 Ma) porphyry-related copper mineralisation at Burra. *MESA Journal* 55:19–33. Primary Industries and Resources South Australia, Adelaide.

Queensland Metals Corporation Ltd 1996. *14th annual report 1996*. Queensland Metals Corporation Ltd.

Sceats M and Hodgson P 2018. *Improved pathogen inhibitor*, US Patent Application 20180007913. United States Patent and Trademark Office, viewed 2 January 2019, <https://patents.justia.com/patent/20180007913>.

Sceats MG, Horley CJ and Richardson P 2007. *System and method for the calcination of minerals*, US Application Number 12/295,468, Patent US 8,807,993 B2, granted 19 August 2014. United States Patent and Trademark Office, Alexandria, US.

Shand MA 2006. *The chemistry and technology of magnesia*. John Wiley & Sons, New Jersey.

Shen Y, Cranfield DE and Knoll AH 2002. Middle Proterozoic ocean chemistry: evidence from the McArthur basin, northern Australia. *American Journal of Science* 302:81–109.

Tosca NJ, Macdonald FA, Strauss JV, Johnson DT and Knoll AH 2011. Sedimentary talc in Neoproterozoic carbonate successions. *Earth and Planetary Science Letters* 306:11–22.

United States Geological Survey 2019. Magnesium compounds. In: *Mineral commodity summaries 2019*. United States Geological Survey, viewed March 2019, <https://doi.org/10.3133/70194932>, pp. 100–101.

Uppill RK 1990. Sedimentology of a dolomite-magnesite-sandstone sequence in the late Precambrian Mundallio Subgroup, South Australia. In JB Jago and PS Moore eds, *The evolution of a late-Precambrian-early Palaeozoic rift complex: the Adelaide Geosyncline*, Special Publication 18. Geological Society of Australia, pp. 105–128.

von der Borch CC and Lock D 1979. Geological significance of Coorong dolomites. *Sedimentology* 26:813–824.

Walling SA and Provis JL 2016. Magnesia-based cements: a journey of 150 years, and cements for the future? *ACS Chemical Review* 116:4170–4204.

Wan Y, Wang X, Chou I-M, Hu W, Zhang Y and Wang X 2017. An experimental study of the formation of talc through $CaMg(CO_3)_2$-SiO_2-H_2O interaction at 100–200°C and vapour-saturation pressures. *Geofluids* 2017, Article ID 3942826. Hindawi, viewed January 2019, <https://doi.org/10.1155/2017/3942826>.

Wietlisbach S 2018. *Latest developments and outlook for magnesium minerals and chemicals*, presentation at Industrial Minerals Congress, Barcelona, 7 June. Fastmarkets IM, viewed 1 March 2019, <http://www.indmin.com/events/download.ashx/document/speaker/E001493/a0ID000000dIDNbMAO/Presentation>.

Wilcock S 1998. Sediment-hosted magnesite deposits. *AGSO Journal of Australian Geology and Geophysics* 17:247–251.

Wilson I 2010. The world of magnesite. *Industrial Minerals* May 2010, pp. 50–67.

Zadeh AMA, Ebner F and Jiang S-Y 2015. Mineralogical, geochemical, fluid inclusion and isotope study of Hohentauern/Sunk sparry magnesite deposit (Eastern Alps/Austria): implications for a metasomatic genetic model. *Mineralogy and Petrology* 109:555–575.

Zedef V, Russell MJ and Fallick AE 2000. Genesis of vein stockwork and sedimentary magnesite and hydromagnesite deposits in the ultramafic terranes of southwestern Turkey: a stable isotope study. *Economic Geology* 85:429–446.

FURTHER INFORMATION

John Keeling
keeling1@bigpond.net.au